EUROPHYSICS LETTERS 15 January 2002

Europhys. Lett., **57** (2), pp. 281–287 (2002)

Generation of the low-density liquid phase of carbon by non-thermal melting of fullerite

A. Cavalleri[1,2], K. Sokolowski-Tinten[1], D. von der Linde[1], I. Spagnolatti[3], M. Bernasconi[3], G. Benedek[3], A. Podestà[4] and P. Milani[1,4]

[1] *Institut für Laser- und Plasmaphysik, Universität Essen - Essen, Germany*
[2] *Materials Sciences Division, Lawrence Berkeley National Laboratory - USA*
[3] *INFM and Dipartimento di Scienza dei Materiali, Università di Milano-Bicocca Via Cozzi 53, I-20125 Milano, Italy*
[4] *INFM and Dipartimento di Fisica, Università di Milano Via Celoria 16, 20133 Milano, Italy*

(received 19 September 2001; accepted 25 October 2001)

PACS. 78.47.+p – Time-resolved optical spectroscopies and other ultrafast optical measurements in condensed matter.
PACS. 81.05.Uw – Carbon, diamond, graphite.
PACS. 71.15.Pd – Molecular dynamics calculations (Car-Parrinello) and other numerical simulations.

Abstract. – By using femtosecond laser excitation, non-thermal melting of fullerite has been experimentally achieved. Because the ultrafast, non-thermal transition occurs approximately at constant volume, the density of the resulting liquid is 25% lower than for non-thermally molten graphite. Tight-binding molecular-dynamics simulations indicate the formation of the low-density liquid phase, composed by *sp*-bonded chains at 7900 K and 7 GPa. The extracted dc resistivity of the liquid (2 mΩ cm) is in agreement with theoretical predictions (2.5 mΩ cm) for the equilibrium low-density phase.

The phase diagram of carbon is, at high temperatures and pressures [1], still poorly understood and difficult to investigate experimentally. In fact, the liquid state cannot be reached at ambient pressures by slow heating of the solid, which sublimes into the gas phase and never reaches the GPa pressures of the melting line. Yet the properties of carbon in this elusive regime are not only interesting in their own right, but have profound implications for a variety of physical phenomena, ranging from the behavior of matter in the interior of planets [2] to the controlled fabrication of materials such as diamond, fullerenes and nanotubes [3]. The extreme states of carbon can, however, be accessed transiently in the laboratory using short-pulse lasers, which allow for rapid heating of the solid phase and high-pressure transients [4, 5]. Further, the use of femtosecond laser pulses is intriguing because the systems can be driven through highly non-equilibrium physical pathways into novel regimes of matter, thereby creating new possibilities for processing applications [6]. An example of these unique pathways is the electronically driven solid-to-liquid transition, or non-thermal melting. This

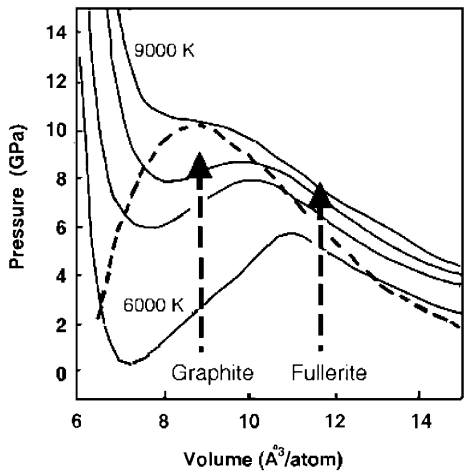

Fig. 1 – Glosli-Ree P-V diagram displaying the two liquid phases of carbon, as calculated in ref. [10]. Full lines: calculated isotherms. Dashed thin line: binodal, limiting the coexistence regime for the two liquid phases. Vertical dashed thick lines: non-thermal melting transitions of high-density graphite and low-density fullerite.

transition is brought about by the lattice de-stabilisation that occurs upon strong electronic excitation [7] and it has been observed in several covalently bonded semiconductors [8]. Isochoric non-thermal melting of graphite was used by Reitze *et al.* [5] to generate and probe the liquid phase of carbon at the approximate density of the solid phase ($2.26\,\mathrm{g/cm^3}$).

The existence of two distinct phases of liquid carbon has been extensively discussed in the literature since 1979 [9]. Most notably, a liquid-liquid first-order phase transition has been clearly identified in recent molecular-dynamics simulations employing empirical interatomic potentials [10] and corroborated by some experimental evidence, albeit indirect [11]. Although the use of empirical classical potentials in the theory may result in sizeable quantitative differences with experiments, the calculated phase diagram reported by Glosli and Ree [10] (see fig. 1) suggests that the isochoric non-thermal melting of graphite achieved by Reitze *et al.* [5], may have resulted in a mixture of the two coexisting liquid phases or in a supercritical fluid. The goal of our work is the observation of the low-density liquid phase, ideally reached by melting a low-density solid phase at quasi-constant volume.

C_{60} crystallizes as a van der Waals solid with a density of $1.68\,\mathrm{g/cm^3}$, 25% lower than graphite. Recently, *ab initio* molecular-dynamics simulations have been performed to study the structural tranformation in fullerite in the first picosecond after intense femtosecond irradiation [12]. These simulations indicate that for sufficiently high electronic excitation, non-thermal fragmentation of the individual C_{60} cages is followed by thermalization into a condensed phase that resembles liquid carbon. However, no experimental evidence of non-thermal melting is to date available for fullerite, despite the indication that this process should lead to the low-density liquid phase (fig. 1) [10].

In the experiments reported here, C_{60} polycrystalline films were grown by thermal sublimation on an optical-grade quarz substrate. A portion of the substrate was masked in order to obtain a film with a sharp edge and to measure the film thickness with an atomic force microscope ($0.98\,\mu\mathrm{m} \pm 10\,\mathrm{nm}$). Ultrafast, time-resolved experiments were performed using pump-probe microscopy, with an interrogating pulse that provided spatially resolved reflec-

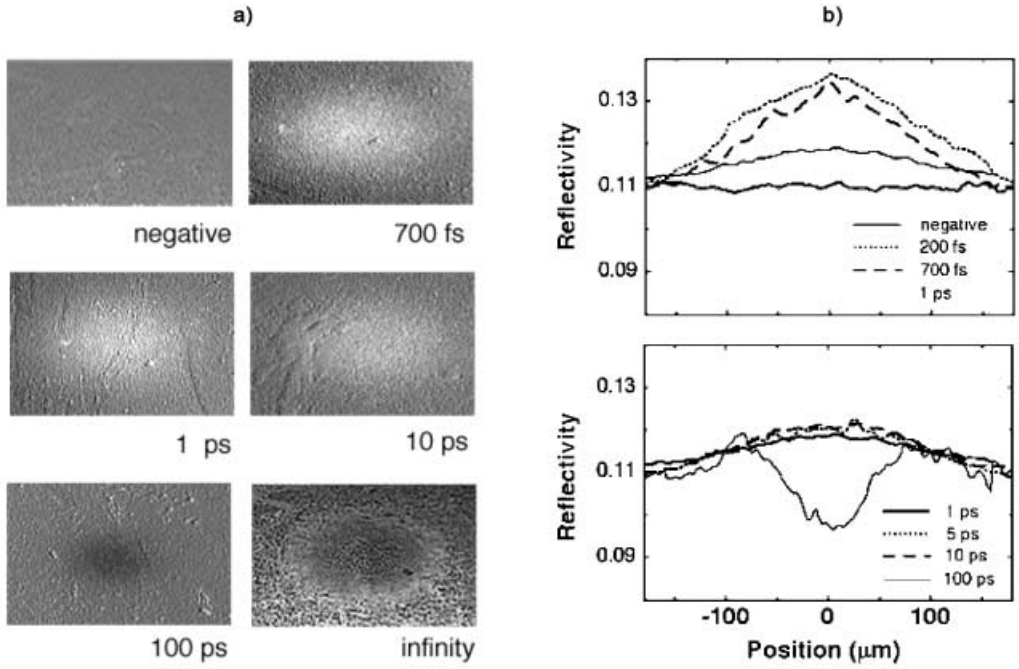

Fig. 2 – Ultrafast, time- and space-resolved images of the melting and ablation process in fullerite. (a) Time-resolved reflectivity images. (b) Lineouts of the reflectivity value across the pumped spot for various time delays.

tivity snapshots of the evolving surface at variable delays after excitation with a pump pulse (fig. 2(a)) [13]. Excitation was obtained with single, 100 fs, 620 nm wavelength p-polarized pulse, impinging onto the film at 45° at a peak fluence of approximately 100 mJ/cm^2. Immediately after absorption of the pump pulse, the reflectivity was observed to rise over a large area. After approximately 200 fs (see fig. 2(b)) the spatially dependent reflectivity indicates that the material is still in an electronically excited state, with its degree of excitation that follows the Gaussian profile of the pump beam. Within few hundred femtoseconds, the reflectivity relaxes toward an intermediate value ($R \approx 0.12$) maintained for 20–30 picoseconds thereafter. At longer time delays the transformed area turns progressively darker, due to hydrodynamic expansion of the generated fluid, eventually resulting in the formation of a crater in the very same region where the transient phase is observed. Plasma formation is not likely to be a cause of the transient, enhanced reflectivity state, because a more pronounced spatial dependence of the optical properties would result (similar to that at 200 fs delay). Also, the expansion of the free electrons would cause rapid ablation, causing a significantly shorter lifetime of this phase [14]. Finally, the threshold for plasma formation should be higher than the $\sim 7 \cdot 10^{11}$ W/cm^2 observed in our experiments [14].

Tight-binding molecular-dynamics simulations [15, 16] were performed for the first 20 picoseconds, in order to clarify the nature of the observed transient state of the material. These calculations extend the scope of the *ab initio* simulations of ref. [12], which were limited to the constant-volume dynamics and covered only the first few hundred femtoseconds following optical excitation. Cells composed by one to four C_{60} molecules were used. As in previous studies, the electrons were assumed to instantaneously thermalize at a given electronic temperature T_{el},

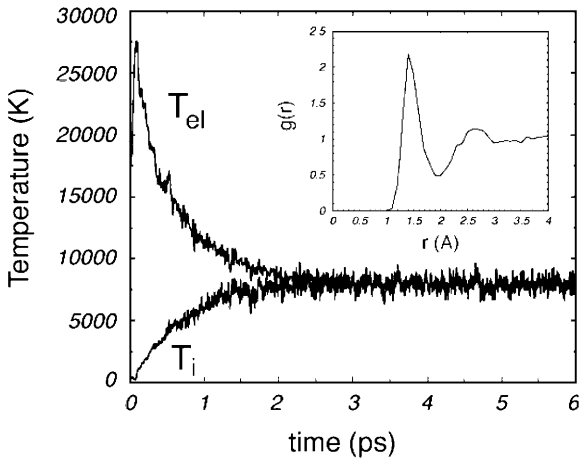

Fig. 3 – Instantaneous ionic and electronic temperature in the simulation with energy absorbed from the laser pulse as large as 3.5 eV/atom, and electronic cooling $\tau_{\mathrm{L}} = 1$ ps, while $\tau_{\mathrm{D}} = \infty$. Inset: Calculated pair correlation function of the high-temperature, low-density liquid phase. The simulations cell contains 240 atoms.

which was increased in time during the first 100 fs, thus mimicking energy absorption (linear in time) from a (square) laser pulse. For an absorbed energy of 3.5 eV/atom the electronically excited state of fullerenes was structurally unstable, giving rise to a liquid with hot electrons and relatively cold ions (~ 1000 K) in few hundred femtoseconds. This liquid corresponds to the same fluid-like phase composed by small chains of twofold-coordinated atoms predicted by the *ab initio* simulations [17]. The electronic temperature was then decreased in time under the combined effect of electron-lattice equilibration and hot-carrier diffusion. Since reliable values for the characteristic times for electron-lattice relaxation (τ_{L}) and hot-carrier diffusion (τ_{D}) are not available for the liquid phase, the relative importance of the two processes was not known precisely.

Guided by what assumed in previous experiments on the ultrafast relaxation of optically excited graphite ($\tau_{\mathrm{D}} \gg \tau_{\mathrm{L}}$) [18], we performed a first set of simulations, neglecting carrier diffusion ($\tau_{\mathrm{D}} = \infty$) and varying τ_{L} over the range 1–6 ps. The energy was subtracted from the electronic system and transferred to the lattice as a random increase of the ionic velocities, in such a way as to conserve the total energy. Because these simulations were meant to describe the bulk of the material, they were performed at constant volume (at the density of fullerite) until thermalization was achieved. This was done under the assumption that the expansion of the volume of material under consideration would not occur within the simulation time, *i.e.* before an acoustic perturbation had propagated inward from the surface. The evolution in time of the electronic and ionic temperatures is shown in fig. 3 for $\tau_{\mathrm{L}} = 1$ ps. The ions reach 7900 K in $2\tau_{\mathrm{L}}$ (for all values of τ_{L} in the range 1–6 ps), with the system still in a liquid-like phase as indicated by the pair correlation function (see inset, fig. 3). The first peak and first minimum are well defined and the coordination number is 2.0, as expected from the chain-like structure of the liquid, surviving at 7900 K.

The properties of the simulated low-density liquid, obtained here from irradiation of fullerite, are very close to the results of tight-binding simulations by Morris *et al.*, who investigated *equilibrium* liquid carbon at different densities and temperatures [19]. Further, Morris *et al.* report a dc conductivity of 2.5 mΩ cm for liquid carbon at 7000 K and at the density

of fullerite. Our measurement of the sole reflectivity at normal incidence is not sufficient for unique, independent determination of the transient optical constants. However, if one assumes a liquid with the same density of solid fullerite and two electrons per atom contributing to the conductivity (from the simulated twofold coordinated chains), one can fit the reflectivity using a Drude model along the lines reported by Reitze *et al.* in ref. [5]. Under these assumptions, a damping time of 0.01 fs and a dc resistivity of 2 mΩ cm can be extracted from the experiments, showing good agreement with the results of the simulations. Thus, we identify the experimentally observed high-reflecting phase with low-density liquid carbon.

At longer time delays, the 7 GPa internal pressure caused the system to expand indefinitely once the constraint of fixed volume was released and a constant-pressure simulation was switched on. The simulated expansion of the liquid is in qualitative agreement with the darkening of the transformed area and subsequent formation of a crater at the surface, as observed at later time delays in the optical experiments.

A second set of simulations was performed as control by assuming that energy was subtracted from the system only by hot-carrier diffusion assuming that this occurs long before the ions could warm via electron-lattice relaxation ($\tau_{\mathrm{L}} \gg \tau_{\mathrm{D}}$). By choosing τ_{D} in the range 2–6 ps and $\tau_{\mathrm{L}} = \infty$, we observed, on the timescale of $3\tau_{\mathrm{D}}$, the formation of a mainly sp^2-like solid phase ($T_{\mathrm{ions}} \sim 3500$ K). By further cooling the system (both electrons and ions) toward room temperature [20], we observed well-shaped graphitic layers with many pentagon-heptagon pairs as products of resolidification. No significant ablation resulted in this case. Thus, the second set of simulations contrasts with the experimental observations.

In order to verify the possibility of at least partial re-solidification on the surface, as suggested by the latter electronic cooling mechanism (diffusion), pristine and irradiated regions of the film were examined with an AFM operating in contact mode. The topography of the pristine fullerite was characterized by the presence of a coarse granularity (and measured roughness σ was 80 nm) and by protruding large globular structures with micrometer dimensions, typical of a polycrystalline film grown on cold substrate [21]. Close to the threshold for permanent modifications (30 mJ/cm^2), the effect of irradiation was a substantial reduction of the roughness and the disappearance of the globular particles. A finer granularity was measured on the surface ($\sigma = 15$ nm), without any indication of the thermal processes characteristic of irradiation with longer pulses, usually leading to the formation of complex structures on a micrometer scale and larger islands [22]. Above a second threshold of 70 mJ/cm^2 (center of the spot), we observed the formation of a crater, due to ablation of bulk material. This regime corresponds to the range where the transient high-reflectivity phase is observed and is the object of our investigation. Sub-micrometer granularity of intermediate range was observed on the surface of the crater ($\sigma = 35$ nm), with no evidence of thermal annealing. The absence of conventional thermal effects, usually leading to fullerene disruption and to the formation of an amorphous carbon phase [21] in the crater, was conclusively confirmed by MicroRaman characterization, showing no evidence of carbon forms other than fullerite. These results further supported the conclusions drawn from the first set of simulations, with the generation of a hot, low-density liquid followed by complete ablation on a timescale that is too short to thermally affect the volume beneath the melt.

Unlike in graphite [23] and all other linearly absorbing materials previously investigated [24], Newton rings are not observable in the reflectivity images. The presence of Newton rings is generally related to a first-order, liquid-gas phase transition. In fact, upon passage of the expanding fluid through the liquid-gas coexistence region the discontinuity in the speed of sound leads to a sharp density front in the rarefaction wave [24]. The absence of such effect in the fullerite images points toward a smoothly varying rarefaction profile upon ablation into vacuum. This result suggests that the liquid phase at 7900 K and at the density of fullerite

lies above the liquid-gas critical isotherm [25]. However, as yet, too little is known about the liquid-gas critical point to make any quantitative comparison with theory. Also, some caution should be applied in view of the relative coarse pristine surface ($\sigma = 80\,\mathrm{nm}$), which could be responsible for a drop in interference contrast even in the presence of a first-order phase transition.

In summary, we have reported on non-thermal melting of fullerite and generation of the low-density liquid phase of carbon. The experimental results and the tight-binding calculations point toward the following physical picture. After electronic destabilization, electron and ions thermalize and the system relaxes to a hot, *sp*-bonded liquid-like phase, at temperatures of the order of 7900 K and pressures of 7 GPa. The density of this phase is, at the earliest times, close to that of solid fullerite, *i.e.* 11.85 $\mathrm{Å}^3$/atom (as opposed to 9 $\mathrm{Å}^3$/atom for the denser case of graphite). On the phase diagram of Glosli and Ree this *liquid* lies in the region of the low-density liquid phase and below the liquid-liquid critical isotherm. Our work also suggests new possibilities for the experimental study of the phase diagram of carbon. By isochoric melting of various solid phases of carbon, appropriately engineered at chosen densities, information on unexplored regions of the phase diagram could be achieved.

* * *

We thank M. Ferretti and E. Barborini for their help in samples preparation and MicroRaman characterization, and A. Gambirasio for discussions and information. This work has been partially supported by INFM under Advanced Research Project CLASS and by MURST under COFIN99. AC acknowledges support from the HCM program of the European Union during the years 1996-98.

REFERENCES

[1] Whittaker A. G., *Nature*, **276** (1978) 695; *Science*, **200** (1978) 763; Galli G., Martin R. M., Car R. and Parrinello M., *Science*, **250** (1990) 1547.
[2] Robin Benedetti L., Nguyen J. H., Caldwell W. A., Liu H., Kruger M. and Jeanloz R., *Science*, **286** (1999) 100.
[3] Colbert D. T. *et al.*, *Science*, **266** (1994) 1218; Banhart F. and Ajayan P. M., *Nature*, **382** (1996) 433.
[4] Venkatesan T., Jacobson D. C., Gibson J. M., Elman B. S., Braunstein G., Dresselhaus M. S. and Dresselhaus G., *Phys. Rev. Lett.*, **58** (1985) 4374; Malvezzi A. M., Bloembergen N. and Huang C. Y., *Phys. Rev. Lett.*, **57** (1986) 146.
[5] Reitze D. H., Wang X., Ahn H. and Downer M. C., *Phys. Rev. B*, **40** (1989) 11986; Reitze D. H., Ahn H. and Downer M. C., *Phys. Rev. B*, **45** (1992) 2677.
[6] Wang C. Z., Ho K. M., Shirk D. M. and Molian P. A., *Phys. Rev. Lett.*, **85** (2000) 4092.
[7] Stampfli P. and Bennemann K. H., *Phys. Rev. B*, **49** (1994) 7299.
[8] Shank C. V., Yen R. and Hirlimann C., *Phys. Rev. Lett.*, **50** (1983) 454; Saeta P., Wang J. K., Siegal Y., Bloembergen N. and Mazur E., *Phys. Rev. Lett.*, **67** (1991) 1023; Sokolowski-Tinten K., Bialkowski J. and von der Linde D., *Phys. Rev. B*, **51** (1995) 14186.
[9] Ferraz O. A. and March N. H., *Phys. Chem. Liq.*, **289** (1979) 8.
[10] Glosli J. N. and Ree F. H., *Phys. Rev. Lett.*, **82** (1999) 4656.
[11] Togaya M., *Phys. Rev. Lett.*, **79** (1997) 2474.
[12] Gambirasio A., Bernasconi M., Benedek G. and Silvestrelli P. L., *Phys. Rev. B*, **62** (2000) 12644.
[13] Downer M. C., Fork R. L. and Shank C. V., *J. Opt. Soc. Am. B*, **2** (1985) 595.

[14] von der Linde D. and Schüler H., *J. Opt. Soc. Am. B*, **13** (1995) 216.
[15] Xu C. H., Wang C. Z., Chan C. T. and Ho K. M., *J. Phys. Condens. Matter*, **4** (1992) 6047. We also included a long-range van der Waals attraction in the form of an empirical two-body potential for interatomic distances above the cutoff radius (2.6 Å) and approaching a Lennard-Jones potential at larger distances. The interatomic potential has been fitted in such a way as to reproduce the lattice parameter and cohesive energy of fullerite. The distortion of the C_{60} cage with respect to the results of the simple tight-binding model is negligible.
[16] Jeschke H. O., Garcia M. E. and Bennemann K. H., *Appl. Phys. A*, **71** (2000) 361.
[17] Although the electronic structure is better described within the *ab initio* framework than in the tight-binding model, the threshold energy for the C_{60} fragmentation (5.9 eV/atom) given in the *ab initio* study of ref. [15] is most probably an overestimation. In fact, the particular molecular-dynamics technique used there (constant electronic temperature after energy absorption) did not allow for fine-tuning of the energy absorbed from the laser pulse. Moreover, the value of 3.5 eV/atom found here corresponds to the energy necessary to induce the fragmentation *before* energy transfer from the electrons to the ions sets in. Our theoretical approach prevented us from introducing electron-lattice relaxation in the untransformed, insulating phase. This theoretical limitation is most probably the source of an overestimation of the threshold for the formation of the high-reflectivity phase which is experimentally identified in the range 0.7–1 eV/atom.
[18] Seibert K. *et al.*, *Phys. Rev. B*, **42** (1990) 2842.
[19] Morris J. R. *et al.*, *Phys. Rev. B*, **52** (1995) 4138.
[20] Parrinello M. and Rahman A., *Phys. Rev. Lett.*, **45** (1980) 1196.
[21] Manfredini M., Bottani C. E. and Milani P., *J. Appl. Phys.*, **78** (1995) 5945.
[22] Milani P. and Manfredini M., *Appl. Phys. Lett.*, **68** (1996) 1769; Hebard A. F., Zhou O., Zhong Q., Fleming R. M. and Haddon R. C., *Thin Solid Films*, **257** (1995) 147.
[23] Sokolowski-Tinten K., Kudryashov S., Temnov V., Bialkowski J., Boing M., von der Linde D., Cavalleri A., Jeschke H. O., Garcia M. E. and Bennemann K. H., *Ultrafast Phenomena XII*, edited by Elsaesser T., Mukamel S., Murnane M. and Scherer N. (Springer-Verlag) 2000, p. 425.
[24] Sokolowski-Tinten K., Bialkowski J., Cavalleri A., von der Linde D., Oparin A., Meyer-ter-Vehn J. and Anisimov S., *Phys. Rev. Lett.*, **81** (1998) 224.
[25] Cavalleri A., Sokolowski-Tinten K., Schreiner M. and von der Linde D., *J. Appl. Phys.*, **85** (1999) 1.